International Journal of Electronics Communication and Computer Engineering
Volume 8, Issue 3, ISSN (Online): 2249–071X

A Thermodynamic Model of Lithium Nickel Manganese Cobalt Oxide Electrodes

Franz Pichler[1], Katja Fröhlich[2], Simeon Stankov[2], Atanaska Trifonova[2] and Martin Cifrain[1]
[1]Kompetenzzentrum Das virtuelle Fahrzeug Forschungsgesellschaft mbH.(ViF), 8010 Graz, Austria.
[2]Electric Drive Technologies, Austrian Institute of Technology GmbH, 1210 Vienna, Austria.

***Abstract* – A thermodynamic consistent model of lithium intercalation materials is developed and applied to a lithium nickel manganese cobalt oxide (NMC) cathode. The model connects the open-circuit voltage of the working electrode versus lithium to the non-ideal activity of the intercalated lithium. That way a non-ideal correction of the solid particle diffusion in the electrode particles and the exchange current density at the electrode interface can be directly calculated from the open-circuit voltage curve. The model equations are embedded into a single particle model. The advantages of this model against the more common simplifications are validated against experimental data. Altogether only five constant fitting parameters are needed in this model and it is shown that its ability to predict the inner resistance makes it an attractive alternative to the commonly used RC-equivalent circuits.**

***Keywords* – Lithium Ion Battery Modelling, NMC, Single Particle Model, Non-Ideal Behaviour.**

I. INTRODUCTION

Battery modeling is widely used in computer aided engineering processes in order to optimize material compositions or to implement effective control algorithms on battery management systems. As cell tests are not only time consuming but also quite expensive due to abrasion of material and equipment, thermodynamical models are reasonable and meaningful. Additionally, some phenomena inside the cell as well as the behavior of the battery under limited conditions are not measureable. Therefore, modeling lithium ion batteries gives a great insight in the cell and can predict cell behavior and profiles which would not be accessible in another way.

There are many approaches to battery modelling, for example empirical models like RC-equivalent circuits [1][2] or the ARX models [3]. Their parameters are mapped to the state-of-charge (SoC), the temperature (T) and the applied current (I_{app}) via look-up tables. The experimental data used to fit these tables defines the feasible application range for these models and they are not able to predict any behavior out of this range. The ease of application and their fast solution process however, makes them a very popular choice.

Electrochemical models describing the physical transport mechanisms and reaction phenomena in batteries, are capable of predicting the battery behavior in situations not covered by the experimental data as well. The most popular approaches are based on the work of New man et al. [4][5], even though there are also other groups working on battery models, for example Dreyer et al. [6], Latz et al. [7][8] and Bazant et al. [9].

All of the above authors point out the importance of thermodynamic consistency. For the modeling of electrode phenomena like solid diffusion and intercalation reactions, this specifically calls for the treatment of the non-ideal mixture of the intercalated lithium in the working electrodes, which is often neglected by assuming constant diffusion coefficients or ideal exchange current densities.

A good summary on non-ideal material mixture models applied to electrodes is given by Karthikeyan [10]. Here, the basic idea is to fit several model parameters to the open circuit voltage (OCV) of an electrode and there by achieving the non-ideal activity correction terms.

In this work, a lithium nickel manganese cobalt oxide(NMC) electrode model is presented, in which the need for such a mixture model is avoided by directly connecting the Gibbs excess free energy of the mixture to the OCV-curve of the electrode. This way, non-ideal activity correction formulas are achieved without the need for an intermediate mixture model.

These non ideal correction terms are used to calculate the solid state diffusion coefficient and the exchange current density of the NMC electrode. That way, the formulas, describing diffusion and intercalation processes in a thermodynamically consistent manner, are defined, upto a proportionality factor, by measurement of the open-circuit voltage.

A similar model to the one derived was only found in one paper by Christensen et al. [11]. Therefore, it is the authors belief that the analysis of the presented model, and its application to NMC electrodes, which has not been performed yet, contributes to this field and raise awareness for a simple yet effective improvement to the state-of-the-art.

We present one application, that embeds the electrode model into a single particle model [12]. In such an approach the electrolyte, the lithium metal anode and all ohmic resistances are summarized into one ohmic resistor connected to the single particle model. This assumption is feasible for low C-rates and forms a starting point for future refinements and extensions.

As a consequence, the number of parameters in this model is relatively small and therefore easily fit to experimental data as presented in this paper.

II. MODEL

Electrode Model Equations

The main point of the derivation is the non-ideal behavior of the intercalated lithium that influences the electrochemical potential $\tilde{\mu}$, given by

$$\tilde{\mu}= \mu^0 + RT\ln(a) + F\,\phi = \mu^0 + RT\ln(\gamma\xi) + F\,\phi \qquad (1)$$

The deviation from ideal behavior in (1) is expressed by the activity coefficient γ, namely its deviation from 1. The term ξ is the mole fraction of intercalated lithium with respect to the maximal capacity of the intercalation material (0<ξ<1).

This definition corresponds to the intercalation reaction

$$Li^+(l)+e^-(s)+\Theta \Leftrightarrow Li(s). \qquad (2)$$

In equilibrium the sum of the electrochemical potentials of all involved species in (2) is constant, so

$$\mu\tilde{l} + \mu\tilde{e} + \mu\tilde{\Theta} = \mu\tilde{s} \qquad (3)$$

Putting (1) into (3) gives the definition of the electrode open-circuit voltage U_{OCV} as

$$U_{OCV}= E_0 + \frac{RT}{F}\ln\left(\frac{\gamma_\Theta}{\gamma_s}\right) + \frac{RT}{F}\ln\left(\frac{1-\xi_s}{\xi_s}\right) \qquad (4)$$

By standard derivations the solid state diffusion in the electrode particles can be shown to be governed by

$$\frac{\partial c_s}{\partial t} - \nabla.\left(D_S\left(-\frac{F}{RT}\xi_s(1-\xi_s)\frac{\partial U_{ocv}}{\partial \xi_s}\right)\nabla c_s\right) = 0 \qquad (5)$$

Furthermore, the activity coefficients can be used in the Butler-Volmer equation

$$j = i_0(\xi)\left(exp(-\frac{\alpha F}{RT}\eta) - exp(\frac{(1-\alpha)F}{RT}\eta)\right) \qquad (8)$$

Where the exchange current density is then described by

$$i_0 = k a_s^{\alpha} a_\Theta^{(1-\alpha)} = k\exp\left(\frac{F}{RT}\left((\xi-\alpha)U_{OCV} - \int_0^{\xi} U_{OCV}(x)dx\right)\right) \qquad (7)$$

Equations (5), (6) and (7) form the presented model *P*.

In comparison, the commonly used assumptions of constant diffusion and ideal activity in the exchange current density would lead to the equations

$$\frac{\partial c_s}{\partial t} - \nabla.(D_s\nabla c_s) = 0 \qquad (8)$$

and

$$i_0 = k a_s^{\alpha} a_\Theta^{(1-\alpha)} = k\xi^{\alpha}(1\text{-}\xi)^{(1-\alpha)} \qquad (9)$$

which, in combination with Equation (6) form the simplified Model *S*. The presented Model *P* will be compared to the simplified Model *S* on several occasions in this paper.

Model Parameters

Remark that both, the diffusion equation (5) and the action equation (6) with the exchange current density (7), are determined by the measurement of the open-circuit voltage curve $U_{OCV}(\xi)$ of the working electrode and two proportionality factors *Ds* and k_{BV}, which will both be treated as fitting parameters. (1)

Two further fitting parameters are the de-lithiation limit ξ_{min} and the specific charge capacity *q* [$mAhg^{-1}$]. The lithiation level ξ is theoretically determined by the lithiation limits of the material and correlates with the cut-off voltages applied. The fully lithiated NMC electrode theoretically holds 279mAhg−1 which corresponds to the $Li_1Ni_{0.33}Mn_{0.33}Co_{0.33}O_2$ stoichiometry. This gives a maximal lithiation level of ξ_{max}=1. In this work it is assumed that at this composition, the open-circuit voltage is at the lower cut-off voltage of 3 V. The delithated state $Li\xi_{min}Ni_{0.33}Mn_{0.33}Co_{0.33}O_2$ can then be calculated from the discharge capacity *q*, where for example a discharge capacity of q = 140 $mAhg^{-1}$ corresponds to a minimal lithiation stoichiometric factor of ξ_{min} = 0.5 calculated by

$$\xi_{min} = 1 - \frac{q}{279} \qquad (10)$$

One challenge here is, that the practical and the theoretical discharge capacities are not necessarily the same. The theoretical capacity *q* between the applied cut-off voltages of 3V and 4.2V, which is needed for the model, could only be reached in practice by a infinitely long constant-voltage discharge step. Therefore, the variable ξmin and the theoretical capacity *q* are Treated as fitting parameters too. It is shown that their values are close to the expected ones.

The last parameter of the model is the resistance R_0 describing all ohmic resistances involved in the experimental set-up also including the electrolyte conductivity, that can be treated as a linear resistor for relatively low C-rates. Furthermore, it includes the anodic reaction kinetics. The anode is assumed to only develop small over-potentials, for which the reaction kinetics can also be treated as a linear resistance.

III. MEASUREMENT

A standard procedure for slurry preparation at laboratory scale was applied. Cathodes were prepared with a ratio of 80:10:10 between NMC (BASF), carbon black Super P (Timcal) and polyvinylidene flouride binder (MTI), respectively, using N-methyl-2-pyrrolidone (Sigma Aldrich) as solvent. The slurry was milled and mixed for several hours for homogenization and coated on an aluminum current collector via Doctor-Blade method. The dried and pressed electrodes with a final thickness of 40 µm were assembled into type 2032 coin cells for half-cell measurements under inert atmosphere against metallic lithium using LP30 (BASF) as standard electrolyte.

Electrochemical measurements were carried out using Maccor Series 4000 over a cycling range between 3 and 4.2 V. Constant current discharge (DC) and constant current charge experiments, followed by constant voltage charging were performed. The C-rates were varied between 0.5C, 1C

and 2C for each cycle. After reaching the cut-off voltage of 3 V, the cell was allowed to relax for 900 s. Thereafter, charge and discharge pulses with varying C-rate and a pulsing time of 10 s were applied at different SoC-levels (starting from 90% down to 20%). For the galvanostatic intermittent titration technique (GITT) measurements, a pulsing time of 600 s and a current of 0.1C, followed by relaxation time of 2400 s were chosen. The pulses were performed over the whole cycling range for charging and discharging, respectively.

The charge and discharge branches of the GITT experiments were averaged out in order to get a description of the open-circuit voltage independence of the state-of-charge, as shown in Fig. 1.

The GITT measurement is used to estimate the particle diffusion coefficients [13]. For sufficiently small voltage changes and if the voltage versus √t shows expected straight line behavior over the titration step, the diffusion coefficient might be calculated via

$$D = \frac{4}{\pi\tau}\left(\frac{m_B V_M}{M_B S}\right)^2\left(\frac{\Delta U_{OCV}}{\Delta U_t}\right)^2 \qquad (11)$$

Where τ represents the duration of the pulse mB the active mass of the electrode, V_M the molar volume of NMC, M_B the molecular weight of NMC and S the active specific surface area of the electrode. ΔU_{OCV} is the change of the open-circuit voltage while ΔU_t is the change of the cell voltage during the pulse with duration τ neglecting the IR drop, both for the corresponding pulse. Note that the effective reaction surface area S, which is not directly accessible in the fully prepared electrode, forms an unknown scaling factor in Equation (11). The theoretical diffusion coefficient from Equation (5), namely

$$D = D_S\left(-\frac{F}{RT}\xi_s(1-\xi_s)\frac{\partial U_{OCV}}{\partial \xi_S}\right) \qquad (12)$$

Can be calculated from the open-circuit voltage, but also only upto the unknown proportionality factor D_s. Therefore, to compare the diffusion coefficient in Equation (11) to the one predicted by Equation (12), both curves were scaled to an average value of 1. The results are summarized in Figure 1. The shape of the curves are in good agreement which indicates that the theories behind Equations (5) and (11) are also in agreement with each other. The strong decrease of the diffusion coefficient indicates a growing diffusion limitation with decreasing cell voltage.

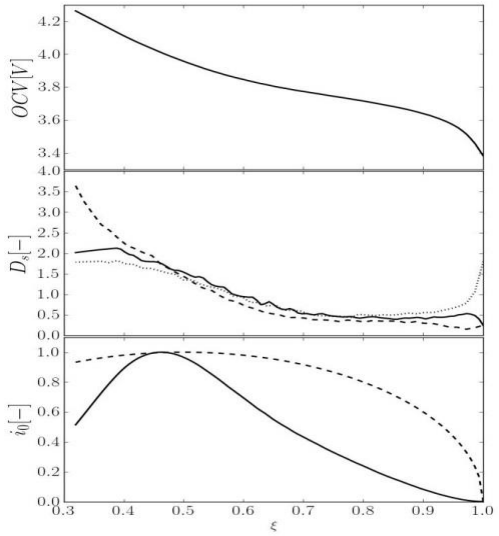

Fig. 1. (top) Open circuit voltage derived from GITT experiment. (middle) The diffusion coefficient as calculated by Equation (11) for the charge (dashed) and discharge (dotted) branch of the GITT experiment and as calculated by Equation (5) from the U_{OCV} curve shown in the top part. (bottom) The exchange current density calculated by the presented model (Equ.(7), solid) and the ideal activity simplification (Equ.(9),dashed).

For the resulting OCV curve, the exchange current density as calculated by Equations (7) and (9) is shown in the bottom part of Figure1. Again, these curves are only determined upto the unknown scaling factor k_{BV}, therefore, they are scaled to a maximal value of one. A big difference can be seen between the two curves. Even though both have their maxima at the lithiation level of $\xi = 0.5$ and both curves decrease to 0 approaching the fully lithiated state, the presented model *P*, utilizing Equation (7), predicts a sharper peak around this maximum than the simplified model *S*, utilizing Equation(9).

IV. Parameterization and Simulation

The parameters R_0, k, ξ_{min}, Q and D_s where fit to the charge/discharge experiments as described above. The voltage profile is shown in Figure3. The relaxation upto 3.6 V after every discharge step, shows how slow the diffusion processes in the fully lithiated cell are, which is in good agreement with the decrease in the diffusion coefficient by the presented model.

Furthermore, the ohmic jump at the beginning and the end of the pause shows that the reaction kinetics are slower at the lithiated electrode too. Again, this coincides with the theory and the commercially applied operating voltage window, which is usually above 3.6*V*.

The parameter fitting was set-up by minimizing the error

$$E = \sqrt{\int_0^T (s(t) - m(t))^2 dx} \qquad (13)$$

Where T is the termination time, $s(t)$ is the simulated cell-voltage and $m(t)$ is the measurement voltage. The measured and simulated voltages are summarized in Figure 3. We would like to emphasize here that the

simulation steps and their termination criteria were performed under the same conditions as the measurement (CD, PAUSE, CCCV). The fact that the simulation switches between these steps nearly at the same time as the experiment is a proof of the quality of the presented model *P*. The model parameters are summarized in Table 1.

Table 1: The resulting values of the parameter fitting with respect to the error function in Equation (13).

Model	D_s $[m^2 s^{-1}]$	k $[Am^{-2}]$	R_0 $[\Omega]$	ξ_{min} $[-]$	q $[mAhg^{-1}]$
P	$1.36 \cdot 10^{-16}$	0.018	6.19	0.32	145.59
S	$2.12 \cdot 10^{-17}$	0.099	6.13	0.30	141.53

Comparing the two model parameter sets, the most obvious difference is that in Model *S* the diffusion coefficient D_S is estimated lower and the exchange current density factor *k* is estimated higher than in Model *P*. This is due to the constant diffusion in Model *S*, that can only map the diffusion limitation in the lower voltage regions by setting a low value for D_S. As a consequence in the higher voltage regions the diffusion limitation is over estimated, which is compensated by an under estimation of the kinetic limitation, i.e. a high value for *k*. This is shown in the under estimated ohmic drops before and after the pause steps. The presented model *P* maps the dependency of the diffusion process on the *SoC* and is therefore able to find a better estimation of the kinetic parameter *k*.

With the fitting parameter values at hand, the second part of the experiment was simulated where charge and discharge pulses, with varying C-rate and 10 s duration, were applied at different SoC levels. Looking at the ohmic drops ΔU(SoC, I) independence of the pulses amplitude I and the So*C* level, an equivalent inner resistance *R*(*I, SoC*) of

$$R(I, SoC) = \frac{\Delta U(I, SoC)}{I} \tag{14}$$

is calculated. The measured and simulated inner resistances, calculated by (14) are shown in Figure 2. Only the ohmic drops are of interest here, not the dynamic step answer of the voltage, because this dynamic part strongly depends on the concentrated electrolyte, especially for the higher current pulses.

Nevertheless, the following results are presented under the hypothesis that the change of ohmic drops with respect to *C*-rate originates in the change of state of the NMC particles, not of the electrolyte or the anode. This is justified by the measured ohmic drops shown in Figure 2. The resistances for the charged electrode, are very small and they do not depend much on the *C*-rate applied. This is a sign that the limiting resistance in this area is linear, and therefore of ohmic or constant nature. This part is governed by the ohmic resistor R_0 to which the single particle model is connected in serial.

For the lower *SoC* levels the resistances are increasing and so does their dependence on the applied *C*-rate. This indicates a non-linear resistance as it is described by the Butler-Volmer Equation (6). It can be seen that the model *P*, fit from the simple scan rate, is capable of predicting the trend of the inner resistance very well.

The NMC electrode shows its best performance in the low lithiated regions where there is still at least one third of the lithium kept in the electrode, assuming that in the operation range only the nickel oxidation [14] is utilized. With growing lithium saturation the resistances are increasing as predicted by the raise of the exchange current density as shown in Figure 1.

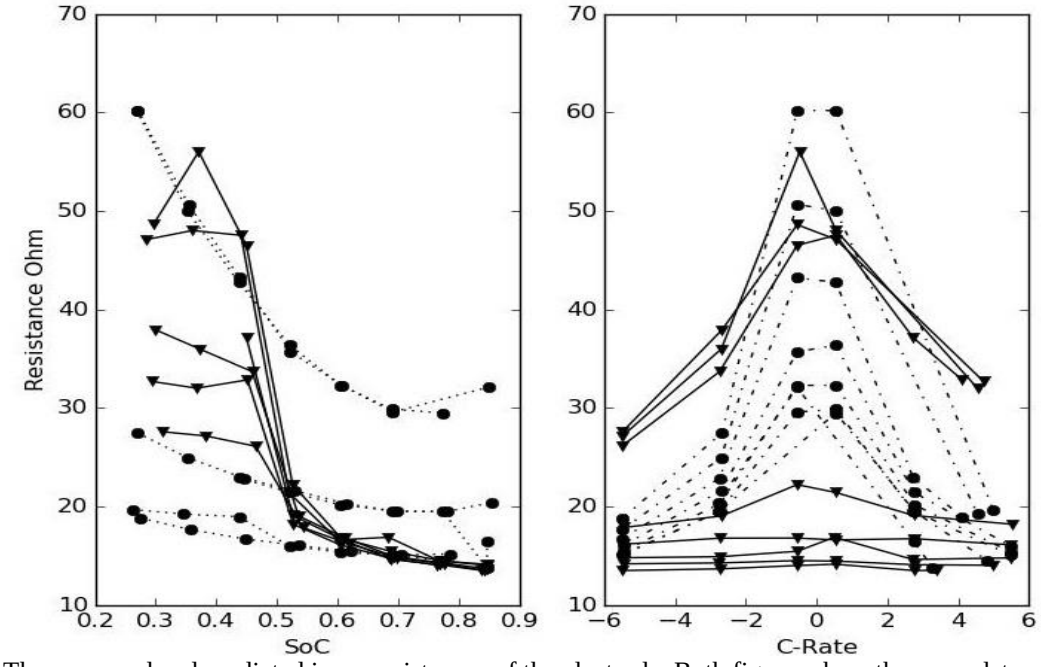

Fig. 2. The measured and predicted inner resistances of the electrode. Both figures show the same data points (dots). (left) The lines connect data points of the same applied C-rate. (right) The lines connect points of the same SoC. The solid lines show measurement data and the dashed lines show predicted values.

The jump in the values at around 60% *SoC* could indicate a change in the intercalation reaction or a general structural change in the electrode itself. This trend could be connected to the saturation of the first oxidation reaction of the nickel.

In order to show the advantage of the presented Model *P* (Equations (5), (6) and (7)) over the simplified Model *S* (Equations(6), (8) and (9)), also the latter set of equations was fitted to the data. The fitting algorithm gave a minimal residual of 6.44 for the presented model (*P*) and a minimal residual of 11.21 for the simplified one (*S*). The resulting simulated voltage curves are compared to the measurement data in Figure 3. The same data is shown over the depth of charge and discharged in Figure 4.

It is easy to see that the simplifications drastically decrease the quality of the model. Especially for the exchange current density there is no good reason to use the simplified version, because in both versions, Model *S* and Model *P*, the exchange current density i_0 is a non-linear term. This means there is no advantage to be expected from the simplification in view of computational cost or usability. Concerning the diffusion coefficient the simplification in Model *S* would bring along some decrease in computational cost, due to the linear nature of Equation (8). However, the ability of Model *P* to predict the increasing diffusion limitation with increasing electrode lithiation should easily outweigh the higher computational cost in most applications. Only if computational cost is the main concern of an application it would make sense to prefer Model *S* over model *P* here.

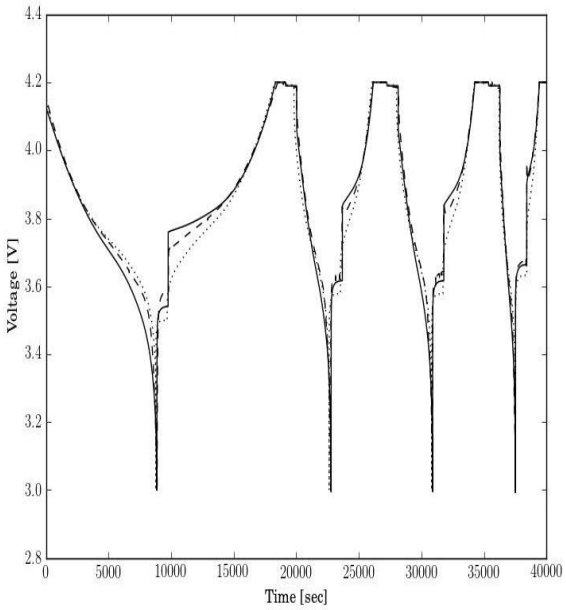

Fig. 3. The dashed line shows the measurement voltage from the rates can experiment. The solid line shows the fit of the presented model. The dotted line shows the fit of the classic model. Especially the relaxation phenomena between the discharge and charge steps, show that the presented model delivers a better description of the solid diffusion and intercalation processes.

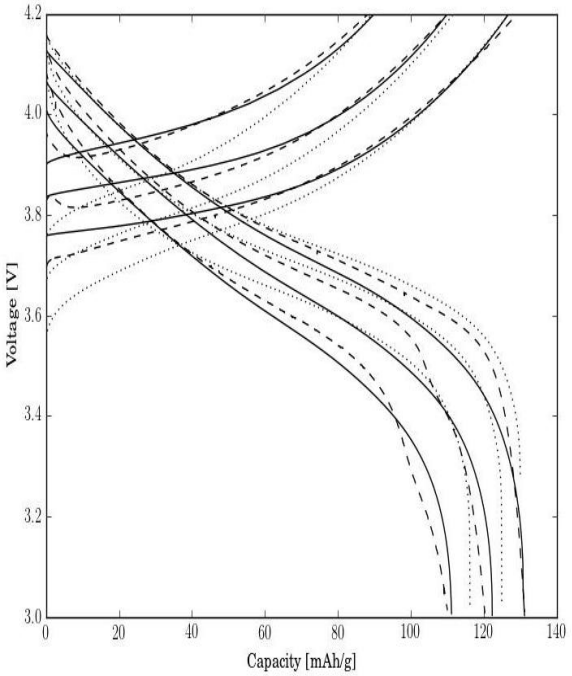

Fig. 4. Charge and discharge voltage over capacity for different C-rates. The dashed lines are the measurement data. The solid lines are the simulation data of the presented model *P*. The dotted lines are the results of the simplified model *S*.

V. Conclusion

A thermodynamically consistent electrode model has been embedded into a single particle simulation. This model is capable of describing the charge, discharge and relaxation phenomena occurring in full rate scans of NMC electrodes upto 2*C*, which governs all the usual applications of NMC electrodes. The authors want to point out here that no adjustment of the slurry preparation or formula was performed and the measurements were solely acting as proof-of-concept regarding the presented model.

Furthermore the inner resistances to pulsed currents have been predicted with out any further adjustment of the model parameters. The predicted exchange current density and the diffusion coefficients are proven to be valid. Therefore we have shown that the presented model is applicable for NMC electrodes.

The whole model is fitted via five constants and therefore easy to apply. Solely CCCV scans are needed for parameterization of the presented thermo dynamical model. Such a model could compete with equivalent circuit models, which are often the first choice in battery management systems and other situation where effective solutions are needed.

In order to be able to analyse the electrode design in more detail, this electrode model has to be embedded in a more sophisticated model that refines the spatial distribution of the involved quantities in the electrolyte and electrode space. The authors are confident that this model delivers a good, easy to apply basis, in order to understand and optimize a broad range of electrodes materials and designs.

ACKNOWLEDGMENTS

This work was performed within the SimPore project, financially supported by the Climate and Energy Fund provided by the Austrian Research Promotion Agency (FFG) partially supported by COMET Program and FFG.

Nomenclature

α	symmetry factor	I	applied current
η	over-potential at electrolyte-electrode interface	i_0	exchange current density
		j	intercalation current density
γ	activity coefficient	k	reaction frequency factor
ϕ	electrical potential	$Li(s)$	intercalated quasi-neutral lithium
τ	pulse duration in GITT		
Θ	vacancy in solid particle phase	$Li_+(l)$	lithium ion in electrolyte phase
ξ	normalized mole fraction of mixture	M_B	Molecular weight of active material
μ	chemical potential	q	electric charge
μ^0	constant standard potential	R	ideal gas constant
$\tilde{\mu}$	electro-chemical potential	R_0	purely ohmic inner resistance of half cell
a	activity		
c_s	concentration of intercalated lithium	S	active specific surface area
		SoC	state of charge
D_s	constant diffusion coefficient	T	temperature
$e_-(s)$	electron in solid particle phase	U_{OCV}	open-circuit voltage vs. Li
E_0	standard equilibrium potential	V_M	molar volume of the active material
F	Faraday's constant		

REFERENCES

[1] Y.-C. Hsieh, T.-D. Lin, R.-J. Chen, H.-Y. Lin, Electric circuit modelling for lithium-ion batteries by intermittent discharging, IET Power Electronics 7 (2014)2672–2677(5).

[2] X.Hu, S. Li, H. Peng, A comparative study of equivalent circuit models for li-ion batteries, Journal of Power Sources 198(2012)359–367.

[3] S. Yuan, H. Wu, C. Yin, State of charge estimation using the extended kalman filter for battery management systems based on the arx battery model, Energies 6(1) (2013)444–470.

[4] M. Doyle, T.F. Fuller, J. Newman, Modeling of galvanostatic charge and discharge of the lithium/polymer/insertion cell, Journal of The Electrochemical Society 140 (6) (1993)1526–1533.

[5] T.F. Fuller, M. Doyle, J. Newman, Simulation and optimization of the dual lithium ion insertion cell, Journal of The Electro chemical Society141(1) (1994)1–10.

[6] W. Dreyer, J. Jamnik, C. Guhlke, R. Huth, J. Moskon, M. Gaberscek, The thermodynamic origin of hysteresis in insertion batteries, Nature Materials 9 (5) (2010) 448–453.

[7] A. Latz, J. Zausch, Thermo dynamic consistent transport theory of li-ion batteries, Journal of Power Sources196(6) (2011)3296–3302.

[8] A. Latz, J. Zausch, Multiscale modeling of lithium ion batteries: thermal aspects, Beilstein Journal of Nano technology 6(2015) 987–1007.

[9] M. Z. Bazant, Theory of chemical kinetics and charge transfer based on non equilibrium thermo dynamics, Accounts of Chemical Research 46(5)(2013)1144–1160.

[10] D. K. Karthikeyan, G. Sikha, R.E. White, Thermo dynamic model development for lithium intercalation electrodes, Journal of Power Sources 185(2)(2008)1398–1407.

[11] J. Christensen, J. Newman, Stress generation and fracture in lithium insertion materials, Journal of Solid State Electrochemistry 10(5)(2006)293–319.

[12] S. Santhanagopalan, Q. Guo, P. Ramadass, R. E. White, Review of models for predicting the cycling performance of lithium ion batteries, Journal of Power Sources 156(2)(2006)620–628.

[13] W. Weppner, R.A. Huggins, Determination of the kinetic parameters of mixed-conducting electrodes and application to the system li3sb, Journal of The Electrochemical Society 124(10)(1977)1569–1578.

[14] M. Labrini, I. Saadoune, A. Almaggoussi, J. Elhaskouri, P. Amoros, Theliyni 0.2mn 0.2co 0.6o2 electrode materials: A structural and magnetic study, Materials Research Bulletin 47(4)(2012)1004–1009.

AUTHORS' PROFILES

Franz Pichler, Mag. Of Numerical Mathematics and Modelling from the Karl-Franzens University Graz, Graz, Austriain 2012. He works at the Kompetenzzentrum Das Virtuelle Fahrzeug Forschungsgesells chaft mb H2012, where he is now a Senior Researcher in the field of battery modeling and simulation.

Recent Publications: Pichler, F., Haase, G.: Finite element method completely implemented for graphic process or units using parallel algorithm libraries. The International Journal of High Performance Computing Applications

Pichler, F., Köster, N.S., Thaler, A.: Thermoelectric simulation of battery-modules with reduced order modeling of linear electrical components, 2016 Proceedings of the 17th International IGTE Symposium, Graz.

Fröhlich, K., Bimashofer, G.,Fafilek, G.,Pichler, F., Cifrain, M., Trifonova A.,: Electrochemical Investigation of Thermodynamic and Transport Phenomena in LP30 Electrolyte with Various Concentrations of Conducting Salt-ECS Trans.201673 (1); Published 15 September 2016

Katja Fröhlich, B.Sc. in Biotechnical Engineering from FHWr. Neustadt, Campus Tulln, 2010, Austria, Dipl. Ing. In Chemical and Pharmaceutical Engineering from Technical University Graz, Graz, Austria, 2013. She worked as a member of the project staff at the Institute of Chemical Engineering and Environmental Technology at the Technical University Grazfrom 2010 to 2011 and is currently working as a Junior Scientist at the Electric Drive Technologies, Austrian Institute of Technology GmbH, 1210 Vienna, Austria, in the field of simulation and material development for battery systems. Recent Publications:

Froehlich, K.,Vasilchina, H.,Stankov, S., Trifonova, A.: Study of transition metal olivines as intercalation host for rechargeable Mg-ion system–in:3rdIndo-Austrian Symposium "Advances in Materials Engineering (AME2016)"

Fröhlich, K., Legotin, E., Trifonova, A.: Estimation of Synthesis Parameters for Large-Scale Production of Lithium Nickel Manganese Cobalt Oxide–in: European Materials Research Society Fall Meeting, Warsaw, 2016(BEST PRESENTATION AWARD)

Fröhlich, K., Bimashofer, G., Fafilek, G.,Pichler, F., Cifrain, M., Tri-fonova A.,: Electrochemical Investigation of Thermodynamic and Transport Phenomena in LP30 Electrolyte with Various Concentrations of Conducting Salt-ECS Trans.201673 (1); Published 15 September 2016